Cellular and Molecular Bioengineering, Vol. 15, No. 6, December 2022 *(© 2022)* pp. 535–551
https://doi.org/10.1007/s12195-022-00742-y

Original Article

Chemotherapy Dose Shapes the Expression of Immune-Interacting Markers on Cancer Cells

Alexander J. Najibi,[1,2] Kerry Larkin,[1,2] Zhaoqianqi Feng,[1,2] Nicholas Jeffreys,[1,2] Mason T. Dacus,[1,2] Yashika Rustagi,[3] F. Stephen Hodi,[3] and David J. Mooney [1,2]

[1]John A. Paulson School of Engineering and Applied Sciences, Harvard University, Cambridge, MA 02138, USA; [2]Wyss Institute for Biologically Inspired Engineering at Harvard University, Boston, MA 02115, USA; and [3]Department of Medical Oncology, Dana-Farber Cancer Institute, Boston, MA 02215, USA

(Received 19 April 2022; accepted 21 September 2022; published online 1 October 2022)

Associate Editor Michael R. King oversaw the review of this article.

Abstract
Introduction—Tumor and immune cells interact through a variety of cell-surface proteins that can either restrain or promote tumor progression. The impacts of cytotoxic chemotherapy dose and delivery route on this interaction profile remain incompletely understood, and could support the development of more effective combination therapies for cancer treatment.
Methods and Results—Here, we found that exposure to the anthracycline doxorubicin altered the expression of numerous immune-interacting markers (MHC-I, PD-L1, PD-L2, CD47, Fas, and calreticulin) on live melanoma, breast cancer, and leukemia cells in a dose-dependent manner *in vitro*. Notably, an intermediate dose best induced immunogenic cell death and the expression of immune-activating markers without maximizing expression of markers associated with immune suppression. Bone marrow-derived dendritic cells exposed to ovalbumin-expressing melanoma treated with intermediate doxorubicin dose became activated and best presented tumor antigen. In a murine melanoma model, both the doxorubicin dose and delivery location (systemic infusion versus local administration) affected the expression of these markers on live tumor cells. Particularly, local release of doxorubicin from a hydrogel increased calreticulin expression on tumor cells without inducing immune-suppressive markers, in a manner dependent on the loaded dose. Doxorubicin exposure also altered the expression of immune-interacting markers in patient-derived melanoma cells.
Conclusions—Together, these results illustrate how standard-of-care chemotherapy, when administered in various manners, can lead to distinct expression of immunogenic markers on cancer cells. These findings may inform development of chemo-immunotherapy combinations for cancer treatment.

Keywords—Chemo-immunotherapy, Tumor immune interaction, Controlled drug release, Doxorubicin.

ABBREVIATIONS

ICD	Immunogenic cell death
APCs	Antigen-presenting cells
BMDCs	Bone marrow-derived dendritic cells
OVA	Ovalbumin

INTRODUCTION

Combination therapies have been a mainstay in cancer treatment for decades. By targeting cancer through distinct pathways, these therapies can potentially minimize the impacts of tumor heterogeneity and reduce off-target toxicities associated with a high-dose monotherapy.[42] Recently, as immunotherapies have taken a center stage in developing cancer treatments, combinations with established modalities such as chemo- and radiotherapy have been explored.[12,15,22,46] These combinations have the potential to both debulk the tumor mass and generate systemic immunity with memory, restraining metastases and providing long-term protection against recurrence.

Cytotoxic chemotherapy has been investigated in combination with immunotherapy due to its ability to release tumor antigen from dying cancer cells for sampling by antigen-presenting cells (APCs)

Address correspondence to David J. Mooney, John A. Paulson School of Engineering and Applied Sciences, Harvard University, Cambridge, MA 02138, USA. Electronic mail: mooneyd@seas.harvard.edu

in situ.[55,70] In addition, certain chemotherapeutic drugs, such as anthracyclines, are reported to induce immunogenic death (ICD) of tumor cells, prompting endogenous antitumor immune responses.[20,33] For example, doxorubicin can induce hallmarks of ICD including cell-surface expression of calreticulin[48] and secretion of ATP[23] and HMGB-1.[4] Anthracyclines such as doxorubicin are commonly used to treat patients with diverse cancers including leukemia and breast cancer, and their influence on antitumor immunity may augment the efficacy of these therapies.[10,17,41] Chemotherapy has now been demonstrated to support the outcomes of immunotherapies including cancer vaccines and immune checkpoint blockade.[21,51,69]

Chemotherapy dosing is based on patient parameters such as total body surface area, with the goal of optimizing a maximally effective dose without toxicity.[26,30] However, even in a monotherapy context, standard dosing may be suboptimal, and the ideal dosing regime for combination with immunotherapy remains unclear.[22,25,26] For example, low doses of common chemotherapies such as cyclophosphamide, 5-fluorouracil, and paclitaxel can deplete suppressive immune cell populations such as regulatory T cells (Tregs) and myeloid-derived suppressor cells, supporting antitumor immune responses.[2] However, high-dose cyclophosphamide is immunosuppressive, and paclitaxel can transiently suppress lymphocyte counts.[6,22] In one clinical trial, metastatic breast cancer patients were treated with combination chemo-immunotherapy consisting of cyclophosphamide, doxorubicin, and a tumor cell vaccine.[19] Only a slim therapeutic window of chemotherapy concentration was noted, above which immune responses were dampened. Thus, ascertaining the appropriate chemotherapy dosing regime is necessary to achieve optimal combination efficacy with immunotherapy.

Live cancer cells express a variety of cell-surface markers that can communicate with immune cells, some that can be recognized by the immune system and bring upon antitumor responses while others are presented for immune evasion.[11] For example, MHC-I complexes presenting tumor antigen to $CD8^+$ T cells are critical for $CD8^+$ T cell recognition and attack of cancer; however, MHC-I downregulation on tumor cells is a response of many cancer types to evade this immune response.[35] Additional surface proteins that can support antitumor immunity are calreticulin and Fas. Calreticulin, as an early cell-surface feature of ICD, can trigger APC phagocytosis, and its expression on leukemic blasts has been implicated in patient survival.[21,32] The tumor necrosis receptor family member Fas, upon its ligation by Fas ligand, triggers apoptotic cell death, and was recently implicated in bystander tumor cell killing by T cells.[60,62] In contrast, other proteins, when presented on cancer cells, can instruct immune cells to not attack the tumor. Cancer cells can present PD-L1 and PD-L2 as ligands for PD-1 on $CD8^+$ T cells to dampen T cell responses to the point of exhaustion.[64] Further, CD47, which acts as a "don't eat me" signal involved in self-recognition, has commonly been found to be upregulated in cancer cells to discourage APC phagocytosis.[39] Among others, these markers influence how immune cells sense and respond to tumor cells, and are common immunotherapy targets.

Here, we investigated the impact of doxorubicin dosing on the induction of ICD of melanoma cells. Doxorubicin has been previously validated to induce apoptosis and canonical ICD markers (calreticulin, HMGB-1, ATP) in melanoma, including the B16-F10 cell line, although typically characterized at a predetermined concentration or timepoint.[13,24,58] This phenomenon has supported therapeutic efforts in melanoma treatment, with novel delivery approaches and drug combinations for doxorubicin under exploration, along with applications for *in situ* vaccination.[1,28,38,40,43] In this work, we characterized the melanoma response to doxorubicin across a range of doses and durations of exposure. Moreover, we studied how doxorubicin dose modulates the expression of immune-interacting markers, which we define as both pro-immune/anti-tumor (e.g., MHC-I, calreticulin, Fas) and immunosuppressive/pro-tumor (e.g., PD-L1, PD-L2, CD47) cell-surface proteins, on live cancer cells both *in vitro* and *in vivo*. We selected these markers, given their importance to cancer immunotherapies, to provide an overview of the immune-interacting profile of live tumor cells. In addition, we assessed how doxorubicin treatment affects cancer antigen presentation and DC activation.

RESULTS

Doxorubicin Induces Immunogenic Cell Death of Melanoma Cells in a Dose-Dependent Manner In Vitro

As expected, doxorubicin demonstrated a dose-dependent response in killing various cancer cell lines (lymphoma, breast cancer, and melanoma) over 48 h in tissue culture (Supplementary Fig. 1). EC50 values spanned orders of magnitude, from ~ 50 (B16-F10, TUBO) to ~ 100 nM (4T1) to ~ 1500 nM (E.G7-OVA), consistent with a previous report.[50]

We next characterized the induction of immunogenic cell death (ICD) of melanoma cells by doxorubicin. B16-F10 melanoma cells were treated with doxorubicin-containing media with experimental

timeline detailed in Fig. 1a and analyzed for markers of apoptosis and ICD (Figs. 1b–1d). Cells were seeded to reach ~ 50–70% confluence by the time of analysis (108,000 cells/well for 6 h timepoint, 100,000 cells/well for 12 h timepoint, 56,000 cells/well for 24 h timepoint, 22,000 cells/well for 48 h timepoint), identified through bright-field microscopy of B16-F10 cells seeded at varying cell densities over 4 days (Supplementary Fig. 2). Doxorubicin concentrations at or above 50 nM reliably induced apoptosis over 48 h after treatment (Figs. 1b and 1c). By 6 h, only the highest doxorubicin concentration tested (250 nM) showed evidence of apoptosis induction, and by 12 h and later both the 50 and 100 nM concentrations led to evidence of apoptosis. Unexpectedly, the intermediate 50 nM condition induced the highest level of apoptosis 24–48 h after treatment, possibly due to earlier cell death and destruction at the higher-concentration conditions. Expression of the ICD marker calreticulin was consistent with the apoptosis results (Figs. 1d and 1e). Higher concentrations of doxorubicin initially led to greater upregulation of calreticulin, but by 24–48 h the 50 nM concentration again led to the greatest expression. HMGB-1 secretion in cell supernatant matched these trends, with the most significant increases observed in the 50 nM group over 24–48 h, relative to the number of living cells (Fig. 1f). Visually, live, adherent cancer cells were observed through brightfield microscopy in all concentration groups 48 h after treatment, with minimal changes in cell morphology (Supplementary Fig. 3).

Doxorubicin Alters the Immune-Interacting Profile of Live Cancer Cells

Next, we investigated whether doxorubicin exposure would affect expression of immune-interacting markers on live cancer cells. Three cell lines were tested: B16-F10 melanoma, 4T1 breast cancer, and AS12 acute myeloid leukemia. Each of these lines displayed variable expression of PD-L1, PD-L2, MHC-I, Fas, calreticulin, and CD47 at baseline (Supplementary Fig. 4). Notably, B16-F10 cells tended to express the highest levels of immune-suppressive markers (e.g., PD-L1, PD-L2) and the lowest of pro-immune markers (e.g., MHC-I, Fas).

After treatment, melanoma cells displayed fluorescent signal corresponding to doxorubicin, which increased at higher doses (Supplementary Fig. 5). Doxorubicin treatment broadly altered the expression of immune-interacting markers on B16-F10 cells (Fig. 2). Interestingly, the same intermediate doxorubicin concentration that demonstrated the greatest induction of apoptosis and ICD after 24 h (50 nM) led to significant MHC-I upregulation, which was not observed at higher doses (Figs. 2a and 2b). Intermediate dosing (50–250 nM) also upregulated Fas and PD-L2 on cancer cells (Fig. 2c–f). The immunosuppressive markers PD-L1 and CD47 did not demonstrate this trend, but continued to increase in expression with increasing doxorubicin dose (Figs. 2g–2j). These results were mirrored in the mean fluorescence intensities for each marker, except with PD-L1 which plateaued more quickly by percent positivity than with MFI (Supplementary Fig. 6). Ovalbumin (OVA)-expressing B16-F10 cells, which responded similarly to the parental B16-F10 cell line in terms of viability reduction with doxorubicin exposure (Supplementary Fig. 1), also upregulated calreticulin similarly to the parental B16-F10 cell line after doxorubicin exposure (Supplementary Fig. 7).

Doxorubicin-treated 4T1 breast cancer and AS12 leukemia cells underwent similar changes to B16-F10 cells in their immune-interacting profiles. Notably, all three cell lines displayed the highest MHC-I, Fas, and PD-L2 expression at intermediate doxorubicin concentrations (Figs. 2b, 2d, and 2f; Supplementary Fig. 8a–c). As with the B16-F10 line, PD-L1 and CD47 expression on 4T1 cells increased along with doxorubicin dose, although AS12 cells peaked at intermediate concentrations (Figs. 2h and 2j; Supplementary Fig. 8d and e). The mean fluorescence intensity of each marker broadly matched these trends (Supplementary Fig. 9).

Cancer cell Doxorubicin Treatment Supports Dendritic Cell Activation and Antigen Presentation In Vitro

We next considered how the modulation of immune-interacting markers by doxorubicin might affect the activation state of interacting APCs, such as dendritic cells. We first tested whether residual doxorubicin in the melanoma cell solution might affect their viability or activation. Bone marrow-derived dendritic cells (BMDCs) were cultured in media containing a wide range (10^{-15}–10^{-3} M) of doxorubicin concentrations. Below 10^{-8} M doxorubicin, no changes in DC viability were observed, but viability declined between 10^{-7} and 10^{-6} M (Supplementary Fig. 10a). DC activation (CD80 and MHCII expression) was consistently low below 10^{-10} M doxorubicin, and increased around 10^{-8}–10^{-7} M before dropping off in the few remaining viable cells (Supplementary Fig. 10b and c). From these results, we employed a washing procedure of doxorubicin-treated cancer cells in the subsequent experiments to yield a 10^{7}-fold dilution of any residual doxorubicin (maximum remaining concentration $< 10^{-13}$ M) to avoid affecting BMDC viability or activation.

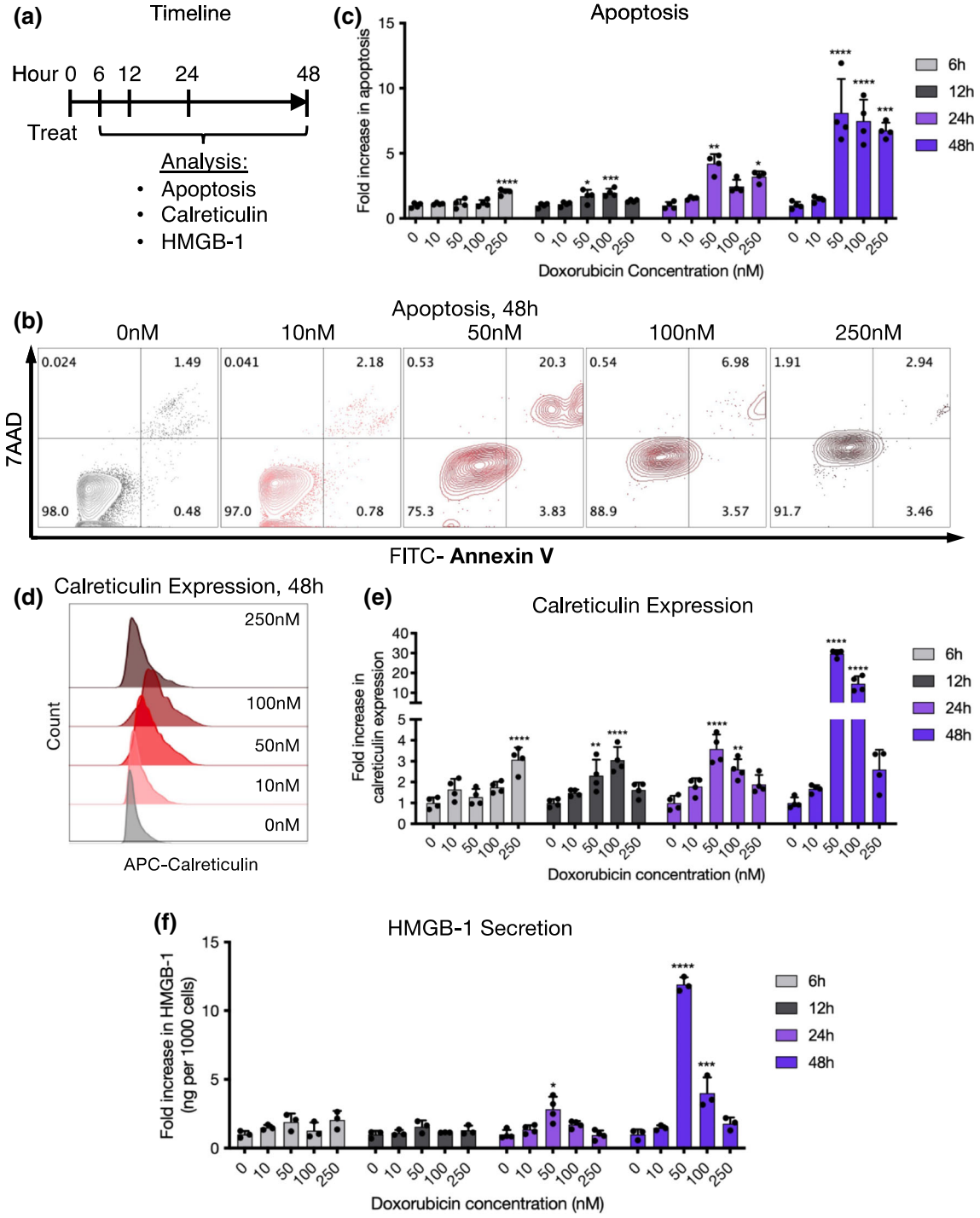

FIGURE 1. Intermediate doxorubicin concentrations effectively induce apoptosis and immunogenic cell death of melanoma cells *in vitro*. (a) Experimental timeline. B16-F10 cells were treated with 0–250 nM doxorubicin and analyzed after 6, 12, 24, and 48 h for apoptosis, calreticulin expression, and HMGB-1 secretion. (b) Representative flow cytometry plots showing apoptosis 48 h after treatment (live cells: Annexin V^- $7AAD^-$, apoptotic cells: Annexin V^+ $7AAD^-$, dead cells: $7AAD^+$). (c) Quantification of apoptosis over time. Fold increase in apoptosis was calculated as the percentage of apoptotic (Annexin V^+ $7AAD^-$) cells in each group divided by the mean of the 0 nM control group at each timepoint. (d) Representative flow cytometry histogram depicting calreticulin expression across groups at 48 h. (e) Quantification of calreticulin expression over time. Fold increase in calreticulin expression was calculated as the percentage of $calreticulin^+$ cells in each group divided by the mean of the 0 nM control group at each timepoint. (f) HMGB-1 secretion over time. Data is plotted as the ng amount of released HMGB-1 per well (assessed through ELISA) relative to the number of live cells recorded through flow cytometry from each well, and normalized to the 0 nM control group at each timepoint.

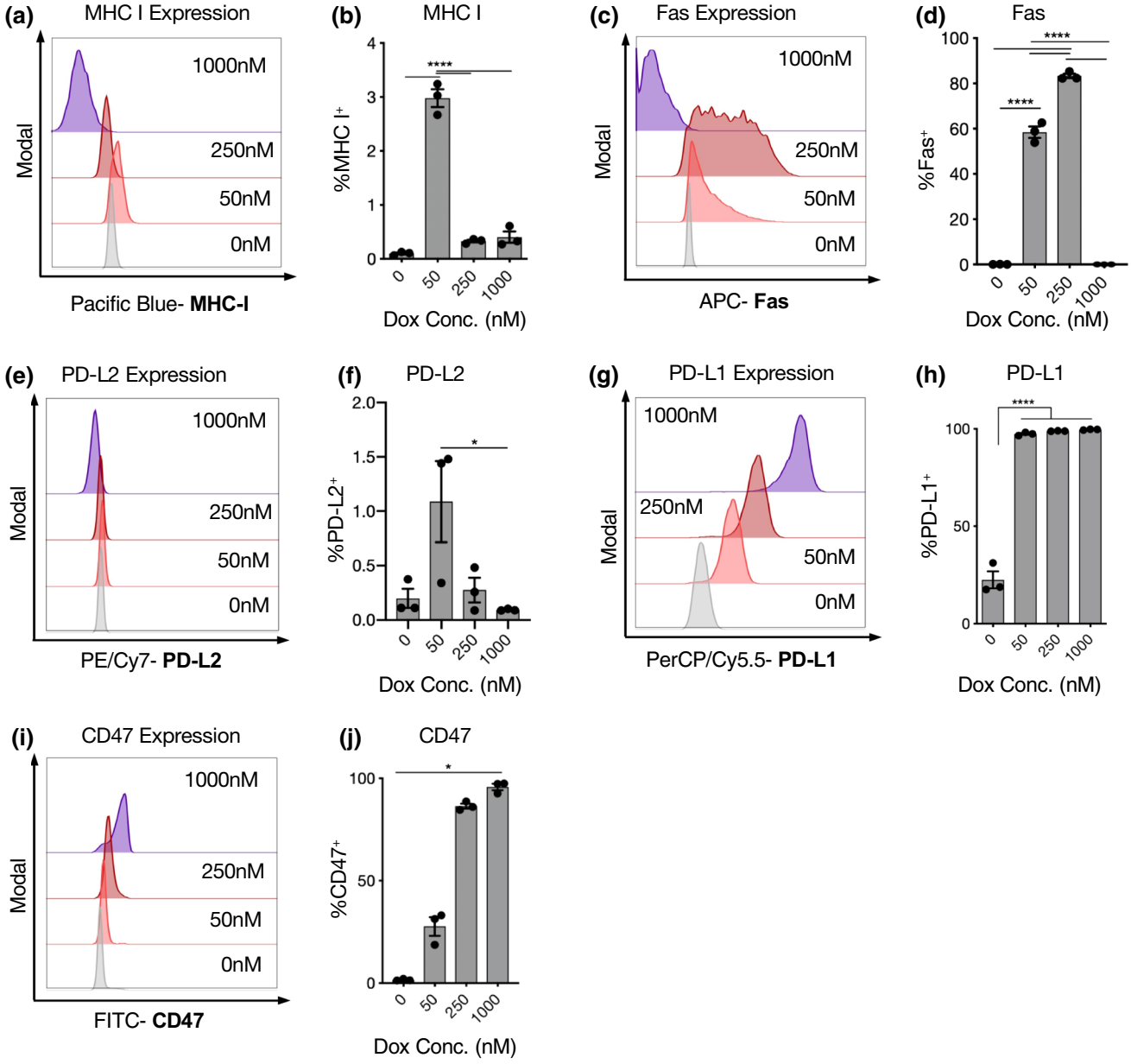

FIGURE 2. Doxorubicin treatment at an intermediate concentration balances expression of immune suppressive and stimulatory markers on melanoma cells *in vitro*. B16-F10 cells were seeded in 12-well tissue culture plates, treated with doxorubicin at a range of concentrations for 24 h, and then collected and analyzed. Representative flow cytometry histograms of MHC-I (a), Fas (c), PD-L2 (e), PD-L1 (g), and CD47 (i). Quantification of expression of MHC-I (b), Fas (d), PD-L2 (f), PD-L1 (h), and CD47 (j).

Using this method, BMDCs were cocultured with doxorubicin-treated B16-mCherry cells. Interestingly, compared to pure BMDCs, BMDCs that had been cocultured with untreated or 10 nM doxorubicin-treated B16-mCherry cells presented a reduced activation state, with lowered expression of CD86 and MHCII (Figs. 3a and 3b, Supplementary Fig. 11a and b). However, B16-mCherry cells that had been pretreated with 50–100 nM doxorubicin did not have this effect, and when the concentration was increased to 250–1000 nM, BMDC activation increased over the control (non-cocultured) cells.

The ability of doxorubicin treatment to improve tumor antigen presentation was next assessed using B16-F10 cells expressing the model antigen OVA. B16-OVA cells treated with doxorubicin over 24 h increased their expression of SIINFEKL-MHC-I complexes, consistent with the previously observed increase in MHC-I expression on parental B16-F10 cells after doxorubicin exposure (Fig. 3c). BMDCs were cocultured with dox-

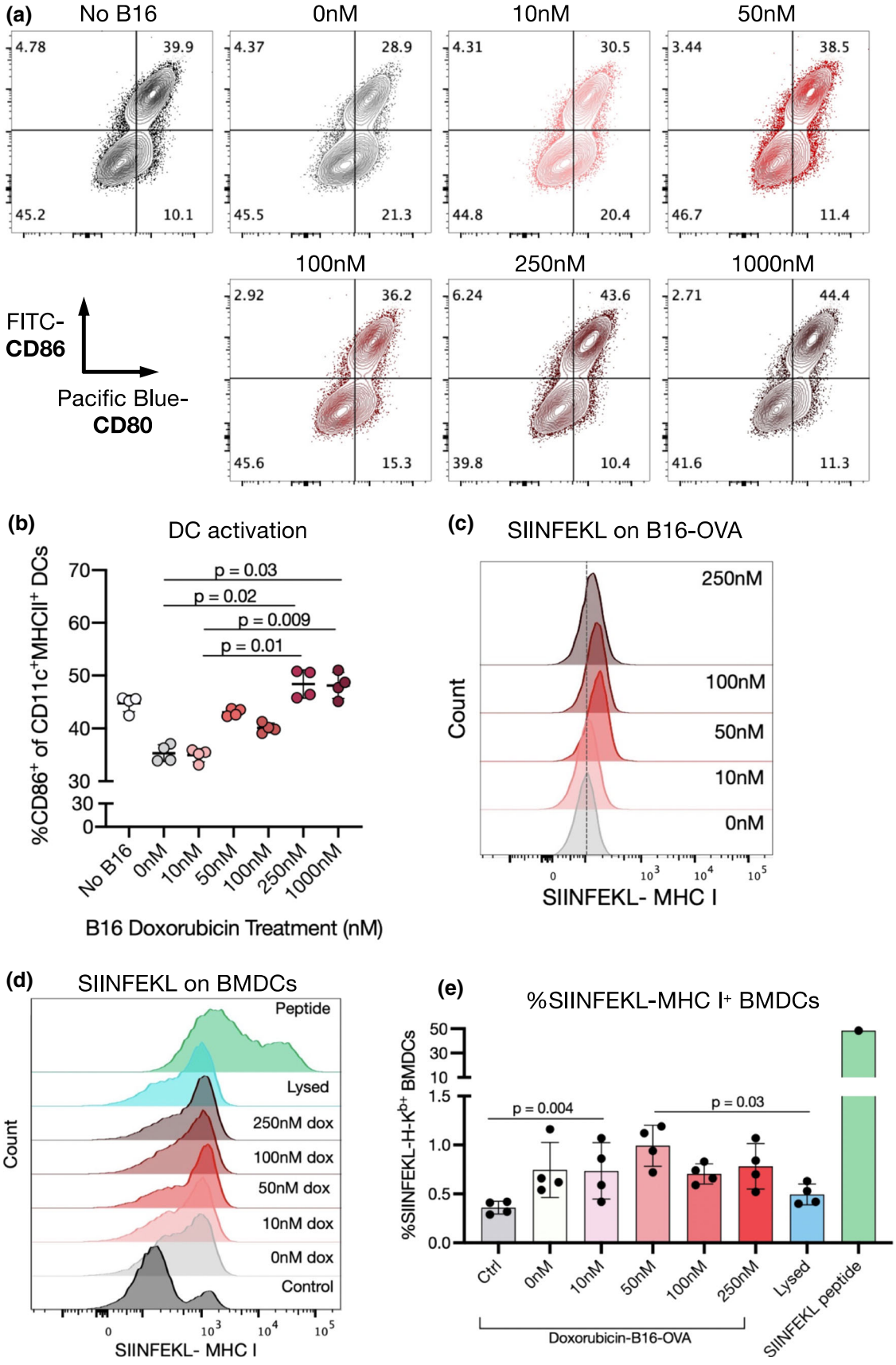
(a)
No B16
0nM
10nM
50nM
4.78
39.9
45.2
10.1
4.37
28.9
45.5
21.3
4.31
30.5
44.8
20.4
3.44
38.5
46.7
11.4
100nM
250nM
1000nM
2.92
36.2
45.6
15.3
6.24
43.6
39.8
10.4
2.71
44.4
41.6
11.3
FITC-
CD86
Pacific Blue-
CD80
(b)
DC activation
%CD86+ of CD11c+MHCII+ DCs
p = 0.03
p = 0.02
p = 0.009
p = 0.01
No B16
0nM
10nM
50nM
100nM
250nM
1000nM
B16 Doxorubicin Treatment (nM)
(c)
SIINFEKL on B16-OVA
250nM
100nM
50nM
10nM
0nM
Count
SIINFEKL- MHC I
(d)
SIINFEKL on BMDCs
Peptide
Lysed
250nM dox
100nM dox
50nM dox
10nM dox
0nM dox
Control
Count
SIINFEKL- MHC I
(e)
%SIINFEKL-MHC I+ BMDCs
%SIINFEKL-H-Kb+ BMDCs
p = 0.004
p = 0.03
Ctrl
0nM
10nM
50nM
100nM
250nM
Lysed
SIINFEKL peptide
Doxorubicin-B16-OVA

◀FIGURE 3. Doxorubicin treatment of melanoma cells enhances co-cultured DC activation and cancer antigen presentation *in vitro*. (a, b) Bone marrow-derived dendritic cells (BMDCs) were cocultured for 48 h with B16-mCherry cells that had previously been treated with doxorubicin (0–1000 nM) for 24 h. (a) Representative flow cytometry plots of CD86 and CD80 expression on $CD11c^{+}MHCII^{+}$ BMDCs. (b) Quantification of CD86-expressing BMDCs. (c-e) B16-OVA cells were treated with doxorubicin (0–250 nM). After 24 h, half of the treated B16-OVA cells were analyzed by flow cytometry. The other half were cocultured with BMDCs for 24 h and then BMDCs were analyzed. (c) Representative flow cytometry plots showing upregulation of SIINFEKL-MHC-I complexes on B16-OVA cells after doxorubicin treatment. (d) Representative flow cytometry plots showing SIINFEKL-MHC-I complexes on BMDCs after coculture with B16-OVA cells. (e) Quantification of SIINFEKL-MHC-I complexes on BMDCs. BMDCs treated with 50 μM SINFEKL peptide in the cell culture medium are also shown as a positive control.

orubicin-treated B16-OVA cells for 24 h and then expression of SIINFEKL-MHC-I complexes on BMDCs was assessed. In all coculture conditions, the proportion of BMDCs presenting OVA peptide increased over non-cocultured BMDCs, but only significantly when B16-OVA cells were pre-treated with 50 nM doxorubicin (Figs. 3d and 3e). BMDCs cocultured with doxorubicin-treated B16-OVA showed higher expression of SIINFEKL-MHC-I complexes than those cultured with lysed B16-OVA cells, but not as high of levels as when BMDCs were exposed to the positive control of SIINFEKL peptide.

The Delivery Route of Doxorubicin Affects the Immune-Interacting Profile of Melanoma Tumors In Vivo

We next tested whether doxorubicin exposure *in vivo* could modulate the expression of immune-interacting markers on tumor cells. We hypothesized that the delivery route (local versus systemic) would have an impact on this profile. A hydrogel carrier was used to achieve local and sustained drug delivery. Hydrogels have been well validated as depots capable of controlled release of drugs including doxorubicin.[36,63] Cryogels, preformed macroporous hydrogels, can be simply injected at various locations.[9,45] In a facile loading method, a concentrated solution of doxorubicin was added dropwise onto dehydrated cryogels, subsequently enabling a continual release of doxorubicin up to 2 weeks after loading (Fig. 4a). Because no difference in drug release was observed when the cryogel-doxorubicin incubation time was varied prior to beginning the release assay, doxorubicin was added immediately (within 1 h) prior to injection in subsequent experiments.

Mice bearing B16-mCherry tumors were injected with blank (unloaded) cryogels, systemic doxorubicin, or local (peritumoral) doxorubicin either as a bolus dose or loaded within a cryogel, each at 7.5 mg/kg (Fig. 4b). Both bolus doxorubicin doses influenced the expression of MHC-I, but also trended towards increasing the expression of immune-suppressive markers such as PD-L1, PD-L2, and CD47 (Figs. 4c–4h). These changes were not observed in tumors treated with gel-delivered doxorubicin. Importantly, both local doxorubicin treatments, but not the systemic treatment, significantly increased tumor calreticulin expression (Figs. 4i and 4j).

The Local Dose of Doxorubicin Affects the Immune-Interacting Profile of Melanoma Tumors In Vivo

Having observed differences between local and systemic dosing of doxorubicin on the immune-interacting profile of tumors, we next assessed the variable of local dose. Mice bearing B16-mCherry tumors were treated with blank cryogels, systemic doxorubicin (7.5 mg/kg), or local doxorubicin delivered from a cryogel at two doses: 7.5 mg/kg (high) or 1 mg/kg (low) (Fig. 5a). Differences in tumor immune-interacting marker expression were observed based both on the delivery location (intraperitoneal vs. peritumoral) and dose (high vs. low). The higher-dose doxorubicin cryogel induced greater calreticulin upregulation than the lower-dose gel (Figs. 5b and 5i). The lower dose gel, however, increased expression of other markers including MHC-I, PD-L1, PD-L2, and CD47, in a manner more similar to the systemic dose (Figs. 5c–5h).

Because tumors were analyzed 3 days after treatment in this experiment and 2 days in the prior, we compared the relative expression in the experimental groups that were used in both experiments. In general, local dosing of doxorubicin did not lead to upregulation of immune-suppressive markers (e.g., PD-L1, PD-L2, CD47), unlike the systemic dosing, but also did not upregulate pro-immune markers (e.g., MHC-I, Fas) to the same extent (Supplementary Fig. 12a–e). Importantly, the highest calreticulin expression was observed in the locally-delivered group across timepoints (Supplementary Fig. 12f). Across experiments, the B16-mCherry tumor line expressed similar levels of immune-related markers to B16-F10 tumors *in vivo*, suggesting relevance of these findings to the parental cell line (Supplementary Fig. 13a–d).

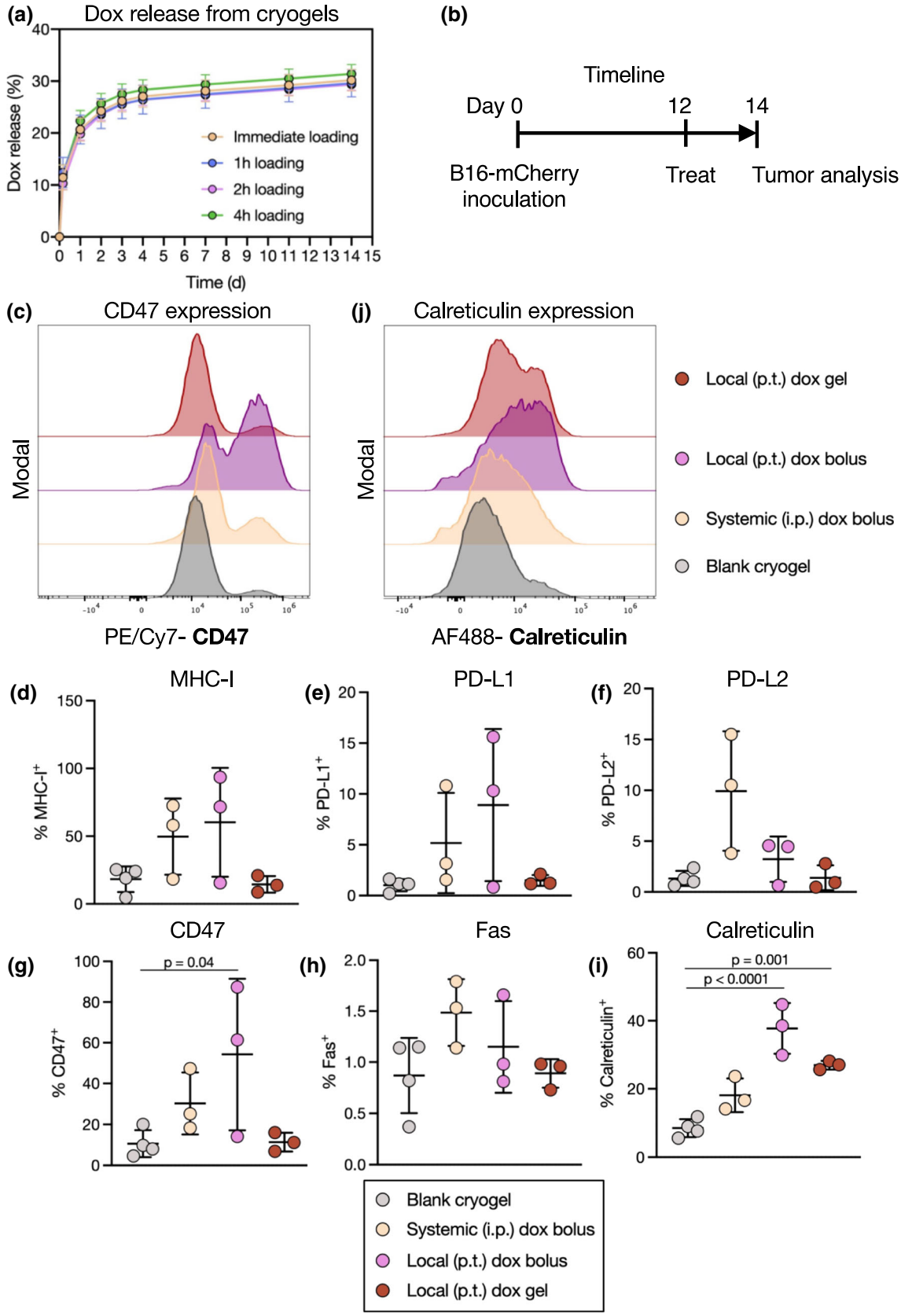
(a)
Dox release from cryogels
Dox release (%)
Time (d)
Immediate loading
1h loading
2h loading
4h loading
(b)
Timeline
Day 0
12
14
B16-mCherry inoculation
Treat
Tumor analysis
(c)
CD47 expression
Modal
PE/Cy7- CD47
(j)
Calreticulin expression
Modal
AF488- Calreticulin
Local (p.t.) dox gel
Local (p.t.) dox bolus
Systemic (i.p.) dox bolus
Blank cryogel
(d)
MHC-I
% MHC-I+
(e)
PD-L1
% PD-L1+
(f)
PD-L2
% PD-L2+
(g)
CD47
p = 0.04
% CD47+
(h)
Fas
% Fas+
(i)
Calreticulin
p = 0.001
p < 0.0001
% Calreticulin+
Blank cryogel
Systemic (i.p.) dox bolus
Local (p.t.) dox bolus
Local (p.t.) dox gel

◀**FIGURE 4. The delivery route of doxorubicin affects tumor immune-interacting marker expression *in vivo*. (a) Doxorubicin was loaded dropwise onto dehydrated cryogels and incubated for 1–4 h prior to beginning the release assay. Release curves of doxorubicin from cryogels over 2 weeks. (b) Experimental timeline and treatment groups. Mice were inoculated with B16-mCherry tumors, treated 12 days later, and tumors were analyzed 2 days after treatment. (c) Representative flow cytometry histograms of CD47 on mCherry$^+$ tumor cells. Quantification of expression of MHC-I (d), PD-L1 (e), PD-L2 (f), CD47 (g), Fas (h), and calreticulin (i) on mCherry$^+$ tumor cells. (j) Representative flow cytometry histograms of calreticulin on mCherry$^+$ tumor cells.**

We next considered how immune-related marker expression may relate to antitumor response and toxicity. Mice treated systemically with a bolus dose of doxorubicin demonstrated a transient, non-significant decline in weight 1–3 days after treatment (Supplementary Fig. 14a). Mice treated with local doxorubicin at low or high doses did not show any significant change in weight 3 days after treatment (Supplementary Fig. 14b). Over the short courses of study (2–3 days of tumor growth after treatment) used in Figs. 4 and 5, no differences in tumor mass at experimental endpoint were noted between groups (Supplementary Fig. 14c). However, expression of immune-related markers MHC-I, PD-L2, CD47, and Fas negatively correlated with tumor size (Supplementary Fig. 14d–i).

To investigate tumor growth kinetics over a longer time period, local doxorubicin dosing was combined with a cryogel-based vaccine delivering granulocyte–macrophage colony-stimulating factor (GM-CSF) and cytosine–guanosine oligodeoxynucleotide (CpG)[45] to treat B16-OVA tumors. Either a low or high dose of doxorubicin trended towards constraining tumor growth relative to blank cryogels, or those containing GM-CSF and CpG without doxorubicin (Supplementary Fig. 15a). In the high-dose doxorubicin group, 1/5 mice rejected tumors and survived tumor-free (Supplementary Fig. 15b).

Doxorubicin Alters the Immune-Interacting Profile of Human Melanoma Cells

The effect of doxorubicin exposure on human cancer cells was next assessed. Five patient-derived melanoma cell lines were treated with doxorubicin over 24 h. Similar to the murine B16-F10 cells, the human cells displayed minimal changes in morphology after treatment with nM dosing of doxorubicin (Supplementary Fig. 16) and doxorubicin uptake was detected through fluorescent signal in each cell line in a dose-dependent manner (Supplementary Fig. 17). The patient-derived cells altered expression of immune-interacting markers (calreticulin, CD47, MHC-I, PD-L1, and Fas) with doxorubicin dose, with variable responses between cell lines (Supplementary Figs. 18–22). Across cell lines, the highest expression of CD47, MHC-I, and PD-L1 was detected in the 0 nM control condition, and generally decreased with increasing doxorubicin concentration (Supplementary Figs. 19–21). Calreticulin and Fas expression tended to peak at intermediate-high doxorubicin concentrations (Supplementary Figs. 18, 22). IFNγ exposure increased the expression of MHC-I and PD-L1, but not calreticulin, in some cell lines, as expected.

DISCUSSION

Doxorubicin capably induced ICD in melanoma cells in a dose and time-dependent manner. Apoptosis and calreticulin expression began as early as 6 h in the culture conditions with the highest doxorubicin concentration, and at lower concentrations increased over 12–48 h. An optimal chemotherapy regime would likely take into account both dose and timing relative to immunotherapy, as considered in previous reports, lending to an ideal therapeutic window.[47,65,67] Unexpectedly, the intermediate 50 nM condition presented the highest apoptosis and ICD marker expression 24–48 h after treatment, suggesting that while a higher dose may more successfully eliminate tumor cells, a lower one may better support immune interaction. Further investigation of the mechanisms underlying these differential effects would likely support the impact of this work. This result matches previous work showing that the optimal doses of mitoxantrone and etoposide chemotherapy for IFNγ^+ CD8$^+$ T cell responses were not the ones resulting in maximal cancer cell death.[58] Optimal combinations of chemo-immunotherapies will likely involve a proper dose and cadence to encourage productive tumor-immune interaction.

The doses found to induce ICD in our *in vitro* studies (10 nM–1 μM) are generally lower than explored in the literature with the B16-F10 melanoma cell line (2.5–50 μM over 24 h[13,58]). However, our EC50 estimation of ~ 50 nM for the B16-F10 cell line matches various studies finding EC50s in the 10 s–100 s nM after 48-–72 h.[18,37,50] This discrepancy may derive from distinct methods of ICD detection (e.g., flow cytometry, immunofluorescence, or functional assays) or incubation times (e.g., consistent versus temporary drug exposure). In our *in vivo* studies, the doses used (1–7.5 mg/kg) are consistent with prior work, typically administering doxorubicin at 1–12 mg/kg in mice.[3,7,29,52] based on findings of 7.5 mg/kg as the maximum tolerated dose in the BALB/c strain.[5] The selections of 7.5 mg/kg as our "high" dose and 1 mg/kg as our "low" dose enabled us to compare

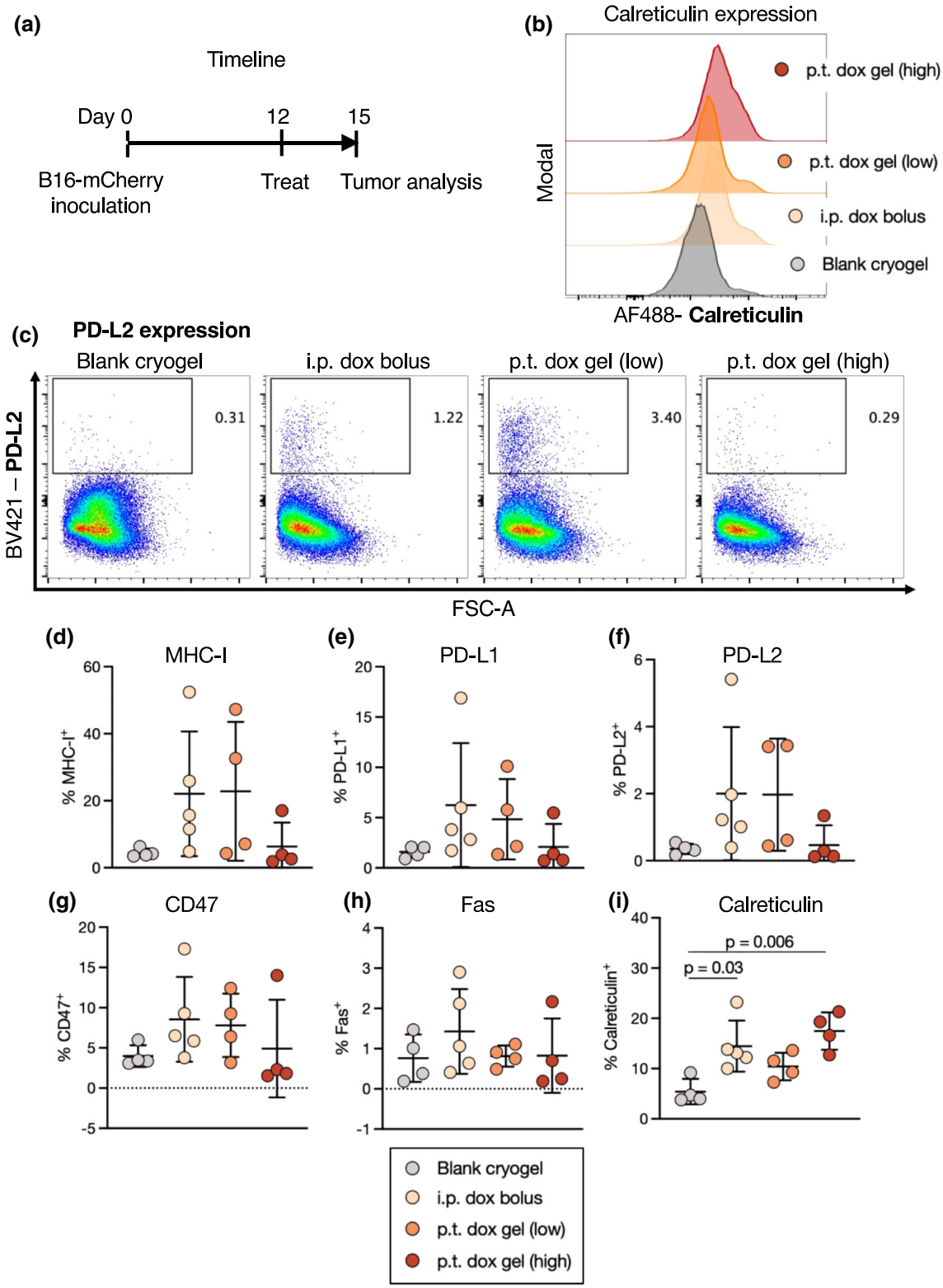

FIGURE 5. The local dose of doxorubicin reshapes tumor immune-interacting marker expression *in vivo*. (a) Experimental timeline and treatment groups. Mice were inoculated with B16-mCherry tumors, treated 12 days later, and tumors were analyzed 3 days after treatment. Doxorubicin was delivered locally delivered from a cryogel at two doses: 7.5 mg/kg (high) or 1 mg/kg (low), or intraperitoneally in a bolus injection at 7.5 mg/kg. Blank cryogels served as controls. (b) Representative flow cytometry histograms of calreticulin on mCherry$^+$ tumor cells. (c) Representative flow cytometry plots of PD-L2 on mCherry$^+$ tumor cells. Quantification of expression of MHC-I (d), PD-L1 (e), PD-L2 (f), CD47 (g), Fas (h), and calreticulin (i) on mCherry$^+$ tumor cells.

across this dose range, with the caveat that the effective dose of doxorubicin at the tumor will be altered by the mechanism of local, controlled release provided by the cryogel. In the clinic, doxorubicin is administered to patients at a ~ 1.9 mg/kg dose in weekly-monthly regimens,[5] and further understanding the impact of repeated dosing (i.e., on–off cycles)[18] versus single dosing on ICD induction could support further therapeutic development.

Live cancer cells treated with doxorubicin underwent significant changes in their expression of key immune-interacting markers. Notably, an intermediate dose balanced anti- and pro-immune marker expression. An optimal dose could theoretically support APC phagocytosis (e.g., maximizing calreticulin while avoiding increasing CD47) and $CD8^+$ T cell recognition and killing (maximizing MHC-I and Fas while avoiding increasing PD-L1). These results are concordant with recent findings that live tumor cells pre-treated with chemotherapy can be injected intratumorally as an adjuvant.[58] In that work, live treated cells, but not dead cells or secreted chemokines/cytokines, stimulated $IFN\gamma^+$ $CD8^+$ T cell responses. These results substantiate our focus on cell-surface markers rather than secreted factors. Moreover, our results may provide a bridge as to why live cells may become immunologically active after chemotherapy exposure, based on their immune-interacting marker expression. The success of other live cell-based therapies such as GVAX, composed of inactivated cancer cells secreting granulocyte–macrophage colony-stimulating factor, may also be supported by these mechanisms.[14,57]

Doxorubicin dosing exerted differential effects on tumor cell lines of different types, suggesting studies are required to optimize the dosing regime for a particular cancer target. For example, PD-L1 expression continued to increase on B16-F10 and 4T1 cells with increasing doxorubicin concentration, while it peaked at an intermediate concentration on a leukemia cell line. The baseline immune-related marker expression on these cell types could potentially inform the extent of an intervention needed to facilitate effective immune interactions.

Chemotherapy pre-treatment of melanoma cells increased the subsequent activation and antigen presentation by cocultured BMDCs. This suggests a functional impact of immune-interacting markers detected on the cancer cells. Importantly, tumor antigen presentation was greatest at the same 50 nM intermediate concentration that best induced immunogenic cell death and pro-immune marker expression of cancer cells. However, DC activation continued to increase with doxorubicin pre-treatment concentration of melanoma cells. This discrepancy might be attributed to the greater extent of dead cell debris and released factors at the higher-concentration conditions.

A notable feature of the *in vivo* studies was the stark difference in baseline immune-related marker expression between melanoma cells from tissue culture and those harvested from tumors—expression of all markers trended to increase *in vivo*. Tumor expression of immune interacting molecules was also highly variable. It is likely that endogenous immune interactions could have driven these differences. PD-L1, PD-L2, and MHC-I can be upregulated by interactions with immune cells and their secreted agents, particularly $IFN\gamma$.[61,64] Fas and CD47 expression are also inducible.[39,62] Previously, chemotherapy itself was found to activate the tumor microenvironment involving IFN signaling, which could serve as a positive feedback loop to further alter the expression of these markers.[31] Better understanding the cellular and molecular drivers of this profile (infiltrating T cell proportions, intratumoral $IFN\gamma$ levels, *etc.*) could account for this variability. Potentially, the higher baseline expression and increased variability *in vivo* may in part account for the more modest changes between treatment groups in this setting.

Doxorubicin, delivered at the same dose either systemically or from a local cryogel, exerted different effects on the tumor immune-interacting profile. Materials-based delivery vehicles for doxorubicin have long been investigated and demonstrated improvements in drug delivery. Notably, Doxil, a PEGylated liposomal doxorubicin, has had an extensive history of use in cancer treatment.[8] Recently, hydrogel-based formulations have delivered chemotherapies adjacent to primary tumors to improve delivery and reduce systemic toxicities.[34,63] Here, doxorubicin delivered from the local cryogel minimally affected expression of suppressive tumor markers (PD-L1, PD-L2, CD47) unlike the systemic dose, but increased calreticulin to a similar extent. Because we found that doxorubicin was released from cryogels *in vitro* over 2 weeks, it is possible that larger effects may be visible beyond 2–3 days of analysis as conducted here, as this is a time when only 20–30% of doxorubicin will have been released from the gel. For example, we previously observed that doxorubicin, conjugated to the tumor-penetrating peptide iRGD and released from a hydrogel, increased tumor macrophage and DC activation and T cell infiltration 11 days later.[63] Additional consideration of the systemic dosing route (i.e., intraperitoneal vs. intravenous) could increase the relevance of these findings for patient translation. Spatial and temporal analyses of the tumor microenvironment (ICD induction, immune cell localization) could further supplement our findings using flow cytometry. T cells and APCs are localized heterogeneously in the B16-F10

tumor microenvironment,[44] and doxorubicin treatment can upregulate calreticulin and increase other ICD markers, also heterogeneously, in primary tumors.[68] Patient melanoma samples also demonstrate heterogeneity in immune and tumor-specific marker expression.[27,53]. Understanding how these profiles evolve over time could allow optimization of strategies for drug delivery, especially with the local delivery approach used in this work. Finally, we found here that the dose of doxorubicin from a hydrogel affected immune-related marker expression *in vivo,* along with influencing tumor growth and mouse survival in a vaccine setting, and a more granular analysis may provide additional insight as to the importance of dose.

Exploration of patient-derived melanoma cell lines supported our findings in the murine models. In this setting, doxorubicin also altered immune-related molecule expression. Interestingly, while the mouse cancer cell lines tended to have low baseline expression of these markers, the 0 nM control condition had highest expression for MHC-I, CD47, and PD-L1 in the clinical samples. This outcome may perhaps be attributed to previous immune exposure of the patient-derived cell lines, and highlights the importance of testing human cells alongside mouse models. Previous reports characterizing the effects of doxorubicin on human tumor cells have also supported the relevance of our key results. Doxorubicin effectively lowered viability of the A375 and MNT-1 melanoma patient-derived cell lines[54] and induced calreticulin upregulation in primary human leukemia and ovarian cancer cells in a time-dependent manner,[20] further indicating that human tumor cells may respond accordingly to the mouse lines used in these studies. In the clinic, calreticulin expression has coincided with effective, anti-leukemia immunity, showcasing how ICD induction may improve therapeutic outcomes in a patient setting.[21,66]

CONCLUSION

In melanoma, breast cancer, and acute myeloid leukemia cell lines, doxorubicin altered the expression of immune-interacting cell-surface proteins. Importantly, treatment of B16-F10 melanoma cells with an intermediate doxorubicin concentration best induced immunogenic cell death, balanced pro-immune and suppressive markers, and supported BMDC antigen presentation. *In vivo*, both the dose and route of administration affected the expression of immune-related markers on cancer cells. These results highlight the importance of chemotherapy exposure on interactions between living cancer cells and immune cells, and support further investigation on chemo-immunotherapy combinations for cancer treatment.

MATERIALS AND METHODS

Murine Cell Lines and Animals

B16-F10 cells (melanoma, derived from C57BL/6J mice) were obtained from ATCC and cultured in DMEM + 10% FBS. mCherry and ovalbumin-expressing B16-F10 cells were obtained from Professor Kai Wucherpfennig's laboratory (Dana-Farber Cancer Institute, Boston, MA). B16-mCherry cells were cultured in DMEM + 10% FBS, and B16-OVA cells were cultured in DMEM + 10% FBS containing 0.4 mg/mL G418 (geneticin, Gibco #10131027). 4T1 cells (triple-negative breast cancer, derived from BALB/c mice) were obtained from ATCC and cultured in DMEM + 10% FBS + 1% penicillin/streptomycin. AS12 cells (acute myeloid leukemia, derived from C57BL/6J mice) were obtained from Professor David Scadden's laboratory (Harvard Stem Cell Institute, Cambridge, MA) as developed in Ref. [59]. These cells were cultured in RPMI containing L-glutamine, 20% FBS, 1% penicillin/streptomycin, 10 μg/mL IL-3, 10 μg/mL IL-6, and 10 μg/mL stem cell factor (R&D Systems, carrier-free). TUBO cells ($Her2^+$ breast cancer, derived from BALB/c mice) were obtained from Professor Yang-Xin Fu's laboratory (University of Texas Southwestern Medical Center, Dallas, TX) and cultured in DMEM + 10% FBS.[49] E.G7-OVA cells (lymphoma, derived from C57BL mice) were obtained from ATCC and cultured in RPMI + 10% FBS + 1% penicillin/streptomycin containing 1 mg/mL G418. 6–8 week-old C57BL/6 J female mice were purchased from Jackson Laboratory (Bar Harbor, ME) and housed with 12 h light–dark cycles and food and water ad libitum. Procedures were compliant with National Institutes of Health and Institutional guidelines and Harvard University's Institutional Animal Care and Use Committee.

In Vitro Doxorubicin Treatment

B16-F10 melanoma cells were seeded in 1 mL media (DMEM + 10% FBS) in 12-well tissue culture plates to reach ~ 50–70% confluence by the time of analysis. From varying the initial seeding densities in the 12-well plate, we ultimately chose 108,000 cells/well for the 6 h timepoint, 100,000 cells/well for the 12 h timepoint, 56,000 cells/well for the 24 h timepoint, and 22,000 cells/well for the 48 h timepoint for the remainder of the *in vitro* doxorubicin experiments (Supplementary Fig. 2). After 24 h, media was replaced with 1 mL fresh media containing doxorubicin at varying concentrations (0 nM, 10 nM, 50 nM, 100 nM, 250 nM, 1000 nM). 6 h, 12 h, 24 h, and 48 h after treatment, cells were detached from plates and the media was

collected and centrifuged at 350 g/5 min to collect cells. Supernatant was collected and stored at − 80 °C for HMGB-1 analysis. For the B16-F10 and B16-OVA comparison experiment, 50,000 cells were seeded in 6-well tissue culture plates and after 24 h were treated with doxorubicin (0 nM, 10 nM and 100 nM) for 48 h before flow cytometry analysis of calreticulin expression.

In Vitro Analysis of Apoptosis and Immune Marker Expression

Cancer cells were collected and washed in 100 μL FACS buffer (PBS + 1% bovine serum albumin + 1% EDTA, Sigma) in a 96-well plate. Samples were resuspended in 100 μL FACS buffer containing relevant antibodies (anti-mouse MHC-I, Fas, PD-L2, PD-L1, CD47, calreticulin as specified in "Flow Cytometry" section), incubated 20 min at 4 °C, then washed in 200 μL cold FACS buffer followed by 200 μL cold PBS. Samples were resuspended in 100 μL Annexin V binding buffer (BioLegend #422201) containing 5 μL FITC-conjugated Annexin V (BioLegend #640906) and 2 μL 7AAD viability staining solution (Invitrogen #00-6993-50) and incubated for 15 min at room temperature. An additional 150 μL of Annexin V binding buffer was added and samples were placed on ice. Flow cytometry was run within 1 h. Doxorubicin has intrinsic fluorescence properties and thus stains were chosen to avoid overlap (i.e., with phycoerythrin channel). EC50 was determined by fitting cell viability curves with log(inhibitor) versus normalized response analysis in GraphPad Prism v6 software to obtain the doxorubicin concentration resulting in 50% viability at 48 h.

HMGB-1 ELISA

HMGB-1 in cell supernatants was quantified using a HMGB-1 ELISA (Tecan #ST5011) per manufacturer protocol. Supernatants from the 6 h and 12 h timepoints were not diluted; supernatants from the 24 and 48 h timepoints were diluted 1:3 in diluent buffer prior to use in the ELISA, with the expectation of greater HMBG-1 release from dying cells and higher concentration at the later timepoints.

Flow Cytometry

Antibodies used in this study include Pacific Blue anti-mouse MHC-I (H-2Kb, C57BL background for B16 and AS12 cells; catalog #116514, clone #AF6-88.5, 1:50 dilution), Pacific Blue anti-mouse MHC-I (H-2K^{d}, BALB/c background for 4T1 cells; catalog #116616, clone #SF1-1.1, 1:50 dilution), PerCP/Cy5.5 anti-mouse PD-L1 (catalog #124,333, clone #10F.9G2, 1:40 dilution), PE/Cy7 anti-mouse PD-L2 (catalog #107213, clone #TY25, 1:80 dilution), Brilliant Violet 421 anti-mouse PD-L2 (catalog # 107219, clone #TY25, 1:80 dilution), APC anti-mouse Fas (catalog #152603, clone #SA367H8, 1:160 dilution), PE/Cy7 anti-mouse CD47 (catalog #127524, clone #miap301, 1:67 dilution), APC anti-mouse CD11c (catalog #117310, clone #N418, 1:80 dilution), PE/Cy7 anti-mouse MHCII (catalog #107629, clone #M5/114.15.2, 1:200 dilution), FITC anti-mouse CD86 (catalog #105005, clone #GL-1, 1:200 dilution), Pacific Blue anti-mouse CD80 (catalog #104723, clone #16-10A1, 1:100 dilution), PE/Dazzle 594 anti-mouse SIINFEKL-H-2Kb (catalog #141612, clone #25-D1.16, 1:50 dilution), APC/Cy7 anti-mouse CD45 (catalog #103115, clone #30-F11, 1:80 dilution), and APC/Cy7 anti-mouse CD31 (catalog #102523, clone #MEC13.3, 1:40 dilution), PE/Cy7 anti-human CD47 (catalog #323114, clone #CC2C6, 1:20 dilution), APC anti-human HLA-A,B,C (catalog #311410, clone #W6/32, 1:20 dilution), Brilliant Violet 421 anti-human PD-L1 (catalog #329714, clone #29E.2A3, 1:20 dilution), Brilliant Violet 605 anti-human Fas (catalog #305628, clone #DX2, 1:20 dilution) (all from BioLegend) and Alexa Fluor 488 and Alexa Fluor 647 anti-calreticulin (catalog #s ab196158 and ab196159, clone #EPR3924, 1:80 dilution, Abcam). Viability was assessed using 7AAD viability staining solution (1:100 dilution, Invitrogen #00-6993-50) or eFluor 780 fixable viability stain (1:1000 dilution, Invitrogen #65-0865-14). Flow cytometry was conducted on BD LSRII and Fortessa flow cytometers and a Cytek Aurora cytometer. Results were analyzed using FlowJo v7.0 and v10.0 software.

BMDC Coculture Experiments

BMDCs were isolated and cultured as previously described.[56] B16-F10 cells (expressing mCherry or OVA protein) were seeded in 12-well tissue culture plates for 48 h and then treated with doxorubicin (0 nM, 10 nM, 50 nM, 100 nM, 250 nM, and 1000 nM, consistent with our previous studies) for 24 h. Cells were scraped, collected into 15 mL tubes, and 10 mL PBS was added. Samples were centrifuged at 350 g for 5 min then 1000 g for 1 min and PBS was removed. The samples were then washed 3× by repeatedly adding 10 mL PBS, centrifuging at 350 g for 5 min, and removing the PBS to achieve an estimated ~ 10^{7}-fold dilution of residual doxorubicin. Collected cells were resuspended in 0.5 mL BMDC media and added to 12-well tissue culture plates. An additional 0.5 mL media containing 2.5×10^{5} BMDCs was added to each well. 24–48 h after BMDC direct coculture with melanoma cells, non-adherent cells were collected by pipetting, washed in FACS

buffer and stained to identify DCs (CD11c, MHCII), activation (CD86, CD80), and tumor antigen presentation (SIINFEKL-H-2 Kb). DCs were also incubated with 50 μM SIINFEKL peptide as a positive control.

Doxorubicin Loading into Cryogels and Release Assay

Click alginate-based cryogels were prepared from norbornene (Nb) and tetrazine (Tz)-modified ultrapure medium viscosity high-guluronic acid (MVG) alginate (NovaMatrix, Sandvika, Norway).[16] The Nb-Tz covalent bond forms by an inverse electron demand Diels–Alder click reaction without additional catalysts. Briefly, Nb and Tz-alginates were dissolved separately to 1.5% wt/vol in DI H_2O and cooled for 10 min at 4 °C. Equal volumes of Nb and Tz-alginate solution were mixed by vortexing and 40 μL of prepolymer mixture was rapidly dispensed onto a pre-cooled Teflon mold, then placed in a − 20 °C freezer overnight. The next day, cryogels were removed from molds after ~ 15 min of thawing. For doxorubicin loading, excess liquid was wicked from cryogels using a Kimwipe and doxorubicin solution was slowly added dropwise onto the dehydrated gels. For a 7.5 mg/kg dose, 0.15 mg of doxorubicin (for 20 g mouse) was added (20 μL of a 7.5 mg/mL doxorubicin solution). To compare the effect of loading time on drug release, doxorubicin was added onto gels 4 h, 2 h, 1 h, or immediately before placing gels into 0.5 mL PBS (gels were incubated at 37 °C during the wait times). PBS was collected and refreshed over the following 2 weeks (after 4 h and 1, 2, 3, 4, 7, 11, and 14 days). The fluorescence signal of doxorubicin was quantified using a Synergy Neo2 plate reader (530/20 excitation, 590/20 emission).

In Vivo Experiments

To compare systemic and local dosing of doxorubicin, 1×10^5 B16-mCherry cells in 100 μL PBS were injected subcutaneously into the upper left flank of C57BL/6 mice. Tumors were allowed to grow for 12 days, then mice were randomized into treatment groups with consistent tumor size distribution (mean and s.d.) and given treatment. Doxorubicin was dissolved in sterile PBS and given as a bolus injection intraperitoneally or peritumorally at 7.5 mg/kg. Doxorubicin was also loaded into a cryogel to deliver at 7.5 mg/kg (high dose) or 1 mg/kg (low dose) and injected peritumorally through a 16G needle by using the vehicle of 200 μL sterile 0.9% saline. Blank cryogels served as controls. Tumors were harvested on day 14, 2 days after the injection of the doxorubicin treatments or day 15, 3 days after the injection of the doxorubicin treatments (as indicated in experimental timelines) for analysis of $mCherry^+$ tumor cells. Distinct timepoints of 2 and 3 days after treatment were selected to characterize the tumor microenvironment over time, and compare the controlled-release cryogel system to the bolus injection, which disperses more rapidly.

B16-F10 Comparison In Vivo

1×10^5 B16-F10 cells in 100 μL PBS were injected subcutaneously into the upper left flank of C57BL/6 mice and tumors were collected after 14 days. Live, $CD45^-CD31^-$ cells were stained for MHC-I, PD-L1, CD47, and calreticulin and analyzed through flow cytometry.

Tumor Digestion for Analysis

At experimental endpoint, tumors were collected in 1 mL PBS, placed on ice, and weighed. Tumors were disrupted mechanically using tweezers in an enzymatic digestion solution of RMPI containing 100 U/mL collagenase IV (StemCell Technologies), 50 U/mL hyaluronidase (Sigma), 20 U/mL DNase I (Sigma), and 2% FBS (Gibco). Samples were incubated in a shaking 37 °C water bath for 40 min with periodic vortexing, passed through 70 μm cell strainers into fresh tubes, and washed in PBS + 2% FBS + 2 mM EDTA to obtain a single-cell suspension. Samples were resuspended in 100 μL FACS buffer (PBS + 1% bovine serum albumin + 0.1% sodium azide) containing anti-mouse antibodies (MHC-I, PD-L1, PD-L2, CD47, Fas, calreticulin) at 4 °C for 20 min. Samples were washed in PBS, stained with eFluor 780 fixable viability stain at 4 °C for 20 min, then analyzed through flow cytometry without fixation. Small tumors (< 10 mg) and tumors with poor cell viability ($< 10\%$) were excluded from analysis.

Doxorubicin Toxicity Analysis

1×10^5 B16-F10 cells in 100 μL PBS were injected subcutaneously into the upper left flank of C57BL/6 mice. After 7 days, three groups of mice were (1) left untreated, (2) treated with a single dose of intraperitoneal 7.5 mg/kg doxorubicin, or (3) treated with three doses each of 2.5 mg/kg doxorubicin spaced every 2 days. Mice were weighed prior to treatment and daily following treatment.

Cryogel Vaccine Treatment

2.5×10^5 B16-OVA cells in 100 μL PBS were injected subcutaneously into the upper left flank of C57BL/6 mice. After 8 days, cryogels were injected containing (1) blank, (2) GM-CSF and CpG, (3) GM-CSF, CpG, and 1 mg/kg doxorubicin, or (4) GM-CSF, CpG, and 7.5 mg/kg doxorubicin. Tumor size was

measured externally using calipers, and area calculated $A = (\pi/4) \times \text{length} \times \text{width}$. Mice were euthanized per IACUC protocol according to a cumulative score incorporating body condition, weight loss, and tumor size (tumors ≥ 17 mm in any two dimensions).

Patient-Derived Cell Lines

K028, K029, D513, C415, and C366 human melanomas were obtained from Professor F. Stephen Hodi's laboratory (Dana-Farber Cancer Institute, Boston, MA) and cultured in RPMI + 10% FBS + 1% antibiotic–antimycotic (100X, Gibco #15,240,096). Human melanoma cells were seeded in 1 mL media in 12-well tissue culture plates to reach ~ 70% confluence by the time of analysis (50,000 cells/well for the K028 and K029 cell lines, 75,000 cells/well for the C415 and C366 cell lines, and 100,000 cells/well for the D513 cell line). After 24 h, media was replaced with 1 mL fresh media containing doxorubicin at varying concentrations (0 nM, 10 nM, 50 nM, 100 nM, 250 nM, 1000 nM, and 10,000 nM). 100 ng/mL IFNγ was added in plain media to an additional well over 48 h as a positive control. 24 h after treatment, cells were detached from plates and the media was collected and centrifuged at 350 g/5 min to collect cells for flow cytometry analysis.

Statistical Analyses

Statistical analysis was performed using GraphPad Prism v8. Normally distributed samples were compared using a one-way analysis of variance (ANOVA) with Tukey's post hoc test, or a Kruskal–Wallis test with Dunn's post hoc test otherwise. Data are depicted as mean ± SD. When relevant, ns $p > 0.05$, $*p \le 0.05$, $**p \le 0.01$, $***p \le 0.001$, $****p < 0.0001$. Sample sizes of 3–5 biologically independent animals per group were used for *in vivo* studies, determined empirically from prior publications and input from Harvard University's Institutional Animal Care and Use Committee.

SUPPLEMENTARY INFORMATION

The online version contains supplementary material available at https://doi.org/10.1007/s12195-022-00742-y.

ACKNOWLEDGMENTS

This work was supported by a grant from the NCI/NIH (5R01CA223255). A.J.N. acknowledges a Graduate Research Fellowship from the National Science Foundation. K.L. acknowledges support from the Amgen Foundation. The authors thank Alexander Stafford for providing norbornene and tetrazine-modified alginates.

CONFLICT OF INTEREST

D.J.M. declares the following competing interests: Novartis, sponsored research, licensed IP; Immulus, equity; IVIVA, SAB; Attivare, SAB, equity; Lyell, licensed IP, equity. The other authors declare no competing interests.

RESEARCH INVOLVING HUMAN AND ANIMAL RIGHTS

No human studies were carried out by the authors for this article. All institutional and national guidelines for the care and use of laboratory animals were followed and approved by the appropriate institutional committees.

REFERENCES

1. Aghda, N. H., S. Torres Hurtado, S. M. Abdulsahib, E. J. Lara, J. W. Tunnell, and T. Betancourt. Dual photothermal/chemotherapy of melanoma cells with albumin nanoparticles carrying indocyanine green and doxorubicin leads to immunogenic cell death. *Macromol. Biosci.* 22:1–13, 2022..
2. Alizadeh, D., and N. Larmonier. Chemotherapeutic targeting of cancer-induced immunosuppressive cells. *Cancer Res.* 74:2663–2668, 2014..
3. Alyamkina, E. A., et al. A strategy of tumor treatment in mice with doxorubicin-cyclophosphamide combination based on dendritic cell activation by human double-stranded DNA preparation. *Genet. Vaccines Ther.* 8:7, 2010..
4. Apetoh, L., et al. Toll-like receptor 4-dependent contribution of the immune system to anticancer chemotherapy and radiotherapy. *Nat. Med.* 13:1050–1059, 2007..
5. Aston, W. J., D. E. Hope, A. K. Nowak, B. W. Robinson, R. A. Lake, and W. J. Lesterhuis. A systematic investigation of the maximum tolerated dose of cytotoxic chemotherapy with and without supportive care in mice. *BMC Cancer.* 17:1–10, 2017..
6. Bae, S. H., Y. J. Park, J. B. Park, Y. S. Choi, M. S. Kim, and J. I. Sin. Therapeutic synergy of human papillomavirus E7 subunit vaccines plus cisplatin in an animal tumor model: Causal involvement of increased sensitivity of cisplatin-treated tumors to CTL-mediated killing in therapeutic synergy. *Clin. Cancer Res.* 13:341–349, 2007..
7. Bandyopadhyay, A., et al. Doxorubicin in combination with a small TGFβ inhibitor: A potential novel therapy for metastatic breast cancer in mouse models. *PLoS ONE.* 5(4):e10365, 2010..

[8] Barenholz, Y. Doxil®—the first FDA-approved nano-drug: lessons learned. *J. Control. Release*. 160:117–134, 2012. https://doi.org/10.1016/j.jconrel.2012.03.020..

[9] Bencherif, S. A., et al. Injectable preformed scaffolds with shape-memory properties. *Proc. Natl Acad. Sci. U. S. A.* 109:19590–19595, 2012..

[10] Bianchini, G., J. M. Balko, I. A. Mayer, M. E. Sanders, and L. Gianni. Triple-negative breast cancer: challenges and opportunities of a heterogeneous disease. *Nat. Rev. Clin. Oncol.* 13:674–690, 2016. https://doi.org/10.1038/nrclinonc.2016.66..

[11] Blank, C. U., J. B. Haanen, A. Ribas, and T. N. Schumacher. The "cancer immunogram." *Science (80–)*. 352:658–660, 2016..

[12] Bracci, L., G. Schiavoni, A. Sistigu, and F. Belardelli. Immune-based mechanisms of cytotoxic chemotherapy: implications for the design of novel and rationale-based combined treatments against cancer. *Cell Death Differ.* 21:15–25, 2014. https://doi.org/10.1038/cdd.2013.67..

[13] Casares, N., et al. Caspase-dependent immunogenicity of doxorubicin-induced tumor cell death. *J. Exp. Med.* 202:1691–1701, 2005..

[14] Chiang, C. L. L., F. Benencia, and G. Coukos. Whole tumor antigen vaccines. *Semin. Immunol.* 22:132–143, 2010. https://doi.org/10.1016/j.smim.2010.02.004..

[15] Demaria, S., et al. Radiation dose and fraction in immunotherapy: one-size regimen does not fit all settings, so how does one choose? *J. Immunother. Cancer*. 9:1–15, 2021..

[16] Desai, R. M., S. T. Koshy, S. A. Hilderbrand, D. J. Mooney, and N. S. Joshi. Versatile click alginate hydrogels crosslinked via tetrazine-norbornene chemistry. *Biomaterials*. 50:30–37, 2015. https://doi.org/10.1016/j.biomaterials.2015.01.048..

[17] Döhner, H., D. J. Weisdorf, and C. D. Bloomfield. Acute myeloid leukemia. *N. Engl. J. Med.* 373:1135–1152, 2015..

[18] Eliaz, R. E., S. Nir, C. Marty, and F. C. Szoka. Determination and modeling of kinetics of cancer cell killing by doxorubicin and doxorubicin encapsulated in targeted liposomes. *Cancer Res.* 64:711–718, 2004..

[19] Emens, L. A., et al. Timed sequential treatment with cyclophosphamide, doxorubicin, and an allogeneic granulocyte-macrophage colony-stimulating factor—secreting breast tumor vaccine: a chemotherapy dose-ranging factorial study of safety and immune activation. *J. Clin. Oncol.* 27:5911–5918, 2009..

[20] Fucikova, J., et al. Human tumor cells killed by anthracyclines induce a tumor-specific immune response. *Cancer Res.* 71:4821–4833, 2011..

[21] Fucikova, J., et al. Calreticulin exposure by malignant blasts correlates with robust anticancer immunity and improved clinical outcome in AML patients. *Blood.* 128:3113–3124, 2016..

[22] Galluzzi, L., L. Senovilla, L. Zitvogel, and G. Kroemer. The secret ally: immunostimulation by anticancer drugs. *Nat. Rev. Drug Discov.* 11:215–233, 2012. https://doi.org/10.1038/nrd3626..

[23] Ghiringhelli, F., et al. Activation of the NLRP3 inflammasome in dendritic cells induces IL-1β-dependent adaptive immunity against tumors. *Nat. Med.* 15:1170–1178, 2009..

[24] Gomez-Cadena, A., et al. Immune-system-dependent anti-tumor activity of a plant-derived polyphenol rich fraction in a melanoma mouse model. *Cell Death Dis.* 7:1–12, 2016..

[25] Griggs, J. J., P. B. Mangu, S. Temin, and G. H. Lyman. Appropriate chemotherapy dosing for obese adult patients with cancer: American Society of Clinical Oncology Clinical Practice guideline. *J. Oncol. Pract.* 30(13):1553–1561, 2012..

[26] Gurney, H. How to calculate the dose of chemotherapy. *Br. J. Cancer*. 86:1297–1302, 2002..

[27] Halse, H., et al. Multiplex immunohistochemistry accurately defines the immune context of metastatic melanoma. *Sci. Rep.* 8:1–14, 2018. https://doi.org/10.1038/s41598-018-28944-3..

[28] Huang, F. Y., et al. Induction of enhanced immunogenic cell death through ultrasound-controlled release of doxorubicin by liposome-microbubble complexes. *Oncoimmunology*. 7:1–16, 2018. https://doi.org/10.1080/2162402X.2018.1446720..

[29] Huynh, H., P. K. H. Chow, and K. C. Soo. AZD6244 and doxorubicin induce growth suppression and apoptosis in mouse models of hepatocellular carcinoma. *Mol. Cancer Ther.* 6:2468–2476, 2007..

[30] Kaestner, S. A., and G. J. Sewell. Chemotherapy dosing part I: scientific basis for current practice and use of body surface area. *Clin. Oncol.* 19:23–37, 2007..

[31] Kang, T. H., et al. Chemotherapy acts as an adjuvant to convert the tumor microenvironment into a highly permissive state for vaccination-induced antitumor immunity. *Cancer Res.* 73:2493–2504, 2013..

[32] Kepp, O., et al. Consensus guidelines for the detection of immunogenic cell death. *Oncoimmunology*.3(9):e955691, 2014..

[33] Kroemer, G., C. Galassi, L. Zitvogel, and L. Galluzzi. Immunogenic cell stress and death. *Nat. Immunol.* 23(4):487–500, 2022..

[34] Krukiewicz, K., and J. K. Zak. Biomaterial-based regional chemotherapy: local anticancer drug delivery to enhance chemotherapy and minimize its side-effects. *Mater. Sci. Eng. C*. 62:927–942, 2016. https://doi.org/10.1016/j.msec.2016.01.063..

[35] Lanitis, E., D. Dangaj, M. Irving, and G. Coukos. Mechanisms regulating T-cell infiltration and activity in solid tumors. *Ann. Oncol.* 28:xii18–xii32, 2017..

[36] Li, J., and D. J. Mooney. Designing hydrogels for controlled drug delivery. *Nat. Rev. Mater.* 1(12):16071, 2016..

[37] Licarete, E., et al. Overcoming intrinsic doxorubicin resistance in melanoma by anti-angiogenic and anti-metastatic effects of liposomal prednisolone phosphate on tumor microenvironment. *Int. J. Mol. Sci.* 21(8):2968, 2020..

[38] Liu, J., et al. Co-delivery of IOX1 and doxorubicin for antibody-independent cancer chemo-immunotherapy. *Nat. Commun.* 12:1–17, 2021. https://doi.org/10.1038/s41467-021-22407-6..

[39] Long, K. B., and G. L. Beatty. Harnessing the antitumor potential of macrophages for cancer immunotherapy. *Oncoimmunology*. 2:1–9, 2013..

[40] Makkouk, A., et al. Biodegradable microparticles loaded with doxorubicin and CpG ODN for in situ immunization against cancer. *AAPS J.* 17:184–193, 2015..

[41] Mattarollo, S. R., S. Loi, H. Duret, Y. Ma, L. Zitvogel, and M. J. Smyth. Pivotal role of innate and adaptive immunity in anthracycline chemotherapy of established tumors. *Cancer Res.* 71:4809–4820, 2011..

[42] Mokhtari, R. B., et al. Combination therapy in combating cancer. *Oncotarget*. 8:38022–38043, 2017..

[43] Mu, X., et al. Doxorubicin and PD-L1 siRNA co-delivery with stem cell membrane-coated polydopamine nanopar-

ticles for the targeted chemoimmunotherapy of PCa bone metastases. *Nanoscale*. 13:8998–9008, 2021..
44. Najibi, A. J., et al. Targeting tumor extracellular matrix activates the tumor-draining lymph nodes. *Cancer Immunol. Immunother*. 2022. https://doi.org/10.1007/s00262-022-03212-6..
45. Najibi, A. J., T.-Y. Shih, and D. J. Mooney. Cryogel vaccines effectively induce immune responses independent of proximity to the draining lymph nodes. *Biomaterials*.281:121329, 2022. https://doi.org/10.1016/j.biomaterials.2021.121329..
46. Ngwa, W., O. C. Irabor, J. D. Schoenfeld, J. Hesser, S. Demaria, and S. C. Formenti. Using immunotherapy to boost the abscopal effect. *Nat. Rev. Cancer*. 18:313–322, 2018. https://doi.org/10.1038/nrc.2018.6..
47. Nowak, A. K., et al. Induction of tumor cell apoptosis in vivo increases tumor antigen cross-presentation, cross-priming rather than cross-tolerizing host tumor-specific CD8 T cells. *J. Immunol*. 170:4905–4913, 2003..
48. Obeid, M., et al. Calreticulin exposure dictates the immunogenicity of cancer cell death. *Nat. Med*. 13:54–61, 2007..
49. Park, S., et al. The therapeutic effect of anti-HER2/neu antibody depends on both innate and adaptive immunity. *Cancer Cell*. 18:160–170, 2010. https://doi.org/10.1016/j.ccr.2010.06.014..
50. Pelczynska, M., M. Switalska, M. Maciejewska, I. Jaroszewicz, A. Kutner, and A. Opolski. Antiproliferative activity of vitamin D compounds in combination with cytostatics. *Anticancer Res*. 26:2701–2705, 2006..
51. Pfirschke, C., et al. Immunogenic chemotherapy sensitizes tumors to checkpoint blockade therapy. *Immunity*. 44:343–354, 2016..
52. RotiRoti, E. C., S. K. Leisman, D. H. Abbott, and S. M. Salih. Acute doxorubicin insult in the mouse ovary is cell- and follicle-type dependent. *PLoS ONE*. 7(8):e42293, 2012..
53. Saliba, E., and J. Bhawan. Aberrant expression of immunohistochemical markers in malignant melanoma: a review. *Dermatopathology*. 8:359–370, 2021..
54. Salvador, D., V. Bastos, and H. Oliveira. Hyperthermia enhances doxorubicin therapeutic efficacy against A375 and MNT-1 melanoma cells. *Int. J. Mol. Sci*. 23:1–17, 2022..
55. Shah, N. J., et al. A biomaterial-based vaccine eliciting durable tumour-specific responses against acute myeloid leukaemia. *Nat. Biomed. Eng*. 2020. https://doi.org/10.1038/s41551-019-0503-3..
56. Shih, T.-Y., Injectable, Ultrasound-responsive biomaterials as cancer vaccines. FAS Theses and Dissertations, Harvard University, 2018. http://nrs.harvard.edu/urn-3:HUL.InstRepos:39947191..
57. Soiffer, R. J., K. A. Kooshesh, and V. Ho. Whole tumor cell vaccines engineered to secrete GM-CSF (GVAX). *ImmunoMedicine*. 1:1–11, 2021..
58. Sriram, G., et al. The injury response to DNA damage in live tumor cells promotes antitumor immunity. *Sci. Signal*. 14:eabc4764, 2021..
59. Sykes, D. B., et al. Inhibition of dihydroorotate dehydrogenase overcomes differentiation blockade in acute myeloid leukemia. *Cell*. 167:171-186.e15, 2016..
60. Upadhyay, R., et al. A critical role for fas-mediated off-target tumor killing in t-cell immunotherapy. *Cancer Discov*. 11:599–613, 2021..
61. van Vloten, J. P., et al. Quantifying antigen-specific T cell responses when using antigen-agnostic immunotherapies. *Mol. Ther. Methods Clin. Dev*. 13:154–166, 2019. https://doi.org/10.1016/j.omtm.2019.01.012..
62. Volpe, E., M. Sambucci, L. Battistini, and G. Borsellino. Fas-fas ligand: checkpoint of t cell functions in multiple sclerosis. *Front. Immunol*. 7:1–9, 2016..
63. Wang, H., et al. Biomaterial-based scaffold for in situ chemo-immunotherapy to treat poorly immunogenic tumors. *Nat. Commun*. 2020. https://doi.org/10.1038/s41467-020-19540-z..
64. Wei, S. C., C. R. Duffy, and J. P. Allison. Fundamental mechanisms of immune checkpoint blockade therapy. *Cancer Discov*. 8:1069–1086, 2018..
65. Welters, M. J., et al. Vaccination during myeloid cell depletion by cancer chemotherapy fosters robust T cell responses. *Sci. Transl. Med*. 8(334):334ra52, 2016..
66. Wemeau, M., et al. Calreticulin exposure on malignant blasts predicts a cellular anticancer immune response in patients with acute myeloid leukemia. *Cell Death Dis*. 1:1–9, 2010..
67. Wu, X., Q. M. Feng, Y. Wang, J. Shi, H. L. Ge, and W. Di. The immunologic aspects in advanced ovarian cancer patients treated with paclitaxel and carboplatin chemotherapy. *Cancer Immunol. Immunother*. 59:279–291, 2010..
68. Yang, C., et al. Macrophage membrane-camouflaged shRNA and doxorubicin: a pH-dependent release system for melanoma chemo-immunotherapy. *Research*. 2002:9768687, 2022..
69. Yang, W., et al. In Situ dendritic cell vaccine for effective cancer immunotherapy. *ACS Nano*. 13:3083–3094, 2019..
70. Zhang, F., L. Zhu, X. Huang, G. Niu, and X. Chen. Differentiation of reactive and tumor metastatic lymph nodes with diffusion-weighted and SPIO-enhanced MRI. *Mol. Imaging Biol*. 15:40–47, 2013..